Desalination and Water Treatment
www.deswater.com

doi: 10.1080/19443994.2014.953401

53 (2015) 1516–1531
February

Taylor & Francis
Taylor & Francis Group

Microfiltration of high concentration black tea streams for haze removal using polymeric membranes

Iain S. Argyle, Michael R. Bird*

Department of Chemical Engineering, University of Bath, Bath BA2 7AY, UK, emails: I.S.Argyle@bath.ac.uk (I. S. Argyle); M.R.Bird@bath.ac.uk (M. R. Bird)

Received 8 October 2013; Accepted 31 July 2014

ABSTRACT

Black tea used for ready-to-drink beverages suffers from an inherent haze problem affecting the appeal of products in terms of colour and appearance; the effect also diminishes health-giving properties. Microfiltration of black tea streams up to 10.0 wt.% has been carried out in an attempt to remove this haze as a replacement to current alkali solubilisation methods which can damage the product. The three commercial polysulphone membranes tested show superior haze removal in tea when filtered at ambient temperature, with turbidity values of below 5.0 nephelometric turbidity units (NTU) being recorded for all membranes over all processing conditions tested. In addition, haze reoccurrence has been slowed following membrane filtration, with turbidity values generally remaining below 50 NTU after 4 weeks of cold storage. At the cross flow velocities used for experimentation (0.5–1.5 ms^{-1}), fluxes were below what would be classified as acceptable for industrial applications although flux improvements were shown to be apparent for elevated tangential velocity and transmembrane pressure (4.0 bar) with membrane resistance during filtration dominated by concentration polarisation, a result of the high solids load in the feed. There is a loss of polyphenolics and colour in the permeate product although a trade-off between haze and stability over time and levels of key polyphenolics (responsible for colour and flavour) was expected. The rejection coefficients for polyphenolic species was much greater compared with total solids rejection for all operating conditions. Tea permeate appearance showed strong dependency with operating conditions, which shows the potential for tailoring of tea appearance, a useful capability in terms of maintaining product consistency given natural variability, a result of growing conditions and other factors. Overall, the potential for microfiltration of black tea has been shown to be effective in removing haze with this article highlighting the research efforts required to make this process a scalable industrial possibility.

Keywords: Microfiltration; Black tea liquor; Haze; Polyphenols

*Corresponding author.

Presented at the conference Engineering with Membranes—Towards a Sustainable Future (EWM 2013) Saint-Pierre d'Oléron, France, 3–7 September 2013

1. Introduction

Camellia Sinensis (var. *Sinensis* or *Assamica*) is a tropical or subtropical plant. The tea infusion is the most popular flavoured drink worldwide [1]. Whilst green tea accounts for 70% of the Chinese market and factors strongly in other Asian markets, it is black tea that accounts for around 70% of production and 80% of exports globally [2]. Traditional hot-water tea infusions are consumed by multiple billions of people, though iced-tea beverages (and other ready-to-drink (RTD) teas) serve a substantial proportion of the tea market. Such products have a huge variation from country to country in terms of flavour and strength of tea brews, as well as other flavour variations and functionality achieved through citric acid addition, sugar and sweetener addition, flavouring and vitamin fortification [3].

1.1. Polyphenols in black tea

Polyphenols in black tea are complex molecules responsible for the bitter and astringent taste characteristics, and the concentration of which is correlated positively with higher quality tea infusions [4,5] and enhanced health-giving properties [6–8]. The diverse category of molecules are formed from the principal polyphenolics present in green tea, the catechins (example in Fig. 1(a)), via oxidative polymerisation (via oxidase or peroxidase enzyme activity) to the well-characterised theaflavins (TFs) (Fig. 1(b)), a category of flavan-3-ols of which there are four oligomers in non-, mono- and di-gallated variants. Further enzymatic activity of catechins and TFs via quinone intermediates yields a more disordered group of polyphenols collectively termed thearubigins (TRs). Whilst being substantially speculated upon, a full mechanistic understanding of this group of species is lacking, meaning information about structure, individual component isolation and the characterisation thereof is missing from the literature [1]. Some species of this category have nevertheless been shown to comprise dibenzotropolone and tribenzotropolone structures in both theaflavic and non-theaflavic variations [9].

1.2. Cold-water-soluble tea

The ability to efficiently infuse green, oolong and black tea leaves (from non-, partially or fully fermented leaves, respectively) in cold water to give maximum extraction of key components such as polyphenols is lacking given the sparing solubility of various components [10]. This means that production of cold-water-soluble (CWS) products serves as a convenient solution, where products are sold in powdered form (typically sold by tea manufacturers to blenders) or alternatively packaged as RTD tea products in diluted or concentrated form to be reconstituted with cold water by the consumer.

1.3. Haze formation

The processing of black tea leaves through tea liquor to spray-dried CWS powdered product requires the implementation of a number of unit operations. Typically, black tea leaves prior to extraction are subjected to either the "orthodox" process (which produces a highly aromatic and flavourful tea) or the "cut–tear–curl" process (CTC, producing a strong dark liquor) [11]. Extraction in hot water and de-leafing using meshes and/or centrifugation is then carried out. Upon cooling, an effect known as tea creaming occurs whereby the partitioning of a cold-water-insoluble phase forms, which can eventually precipitate out; the degree of precipitation being related to concentration, pH and time–temperature history [12]. The cream is to the detriment of the product as loss in colour and flavour, as well as appearance and bioactivity, is tarnished.

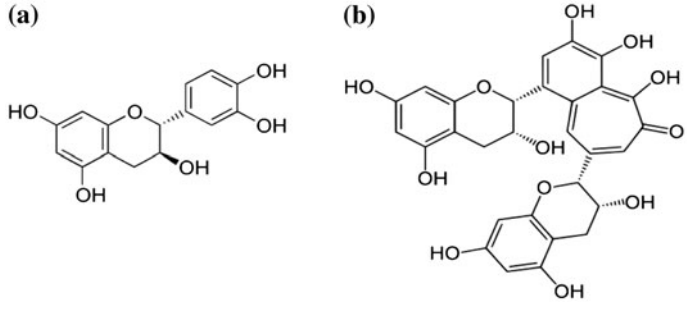

Fig. 1. (a) Catechin, a common green tea polyphenol and (b) theaflavin, a flavan-3-ol present in black tea.

The complexation of polyphenols by association of their galloyl groups, and their limited solubility is said to be a main driver in cream formation [13,14]. Although not an initiator of tea cream and not an essential part, caffeine binds with galloyl groups and tea cream moieties, increasing their mass and density [14]. The presence of Ca^{2+} ions exacerbates cream formation through charge compensation, given the negative charge carried by TFs in solution at the pH of infused tea [13,15]. H^{+} is thought to encourage cream formation by stimulating polyphenols to interact with polysaccharides and nucleophilic groups on proteins [15].

Liang and Xu [15] showed by light scattering that cream particulates showed reasonably consistent sizes, with volume maxima apparent for 0.5-μm particles at pH 1.2, pH 9.0 and most substantially at pH 3.0 (the pH closest to natural tea infusions). At the elevated pH, the peak intensity was lowest showing that solubilisation of cream aggregates is better at high pH. In fact, the irreversible degradation of TFs and consequent formation of their anion or salt result in the loss of their yellow/orange character [15] and create a stewed flavour [16].

1.4. De-creaming

Currently, de-creaming of extracted black tea liquor prior to spray-drying using alkali (NaOH) treatment is a common industrial practice. Aside from the degradation of TFs which adversely affects the appeal of products in terms of appearance and taste, and a reduction in health properties, readjustment of pH with additives such as citric acid causes excessive sodium citrate formation which can further affect the flavour properties of products. Alternative de-creaming methods have been explored such as enzyme treatment [16] although limitations in terms of non-continuous operation (i.e. batch processing) and lengthy times for enzymatic activity present drawbacks. In addition, recovery of enzymes poses further complications.

1.5. Membrane applications

Membrane processes offer a means to remove haze with minimal thermal or chemical impact to the product whilst maintaining a continuous unit operation. There have been a number of studies relating to the membrane filtration of tea for both infusions [17], reconstitutes [18–21] and model component mixtures [22]. The ability of membranes to clarify tea was assessed by Evans et al. [20] when conducting ultrafiltration (UF) of 1.0 wt.% reconstitute at 50˚C. Improvements in the clarity of permeates were recorded for various membrane molecular weight cut-offs and materials (fluoropolymer, polysulphone, regenerated cellulose) and showed improvements in stability over both unfiltered reconstitute and commercial products, with between 62.5 and 73.0% total solids transmission. All of the studies regarding the filtration of black tea liquor reconstitute have centred around the UF operation of low solids concentration feeds (0.5–2.0 wt.%).

Given the aforementioned particulate size of tea cream aggregates, this study aims to show that application of microfiltration (MF) of a high solids stream can be effective in the removal of haze from black tea liquors at ambient temperature by utilisation of membranes as a physical barrier to exclude particulates. Ambient temperature filtration allows for maximum aggregate formation (as haze is formed during cooling) meaning that tea shelf life should be improved over a hot-filtered product. Utilisation of a high solids load (10.0 wt.%) means that effective membrane processes can be carried out at a higher process intensity, the result of such an elevated feed concentration resulting in reductions in terms of water usage, cleaning solution usage and capital expenditure.

Filtration fluxes, stream compositions, turbidity and colour of permeates, resistances for concentration polarisation (CP), reversible and irreversible fouling as well as an insight into mechanisms of pore blocking and mass transfer are assessed as complimentary techniques in order to analyse and discuss the filtration behaviour.

1.6. Pore-blocking mechanisms

Power-law pore-blocking mechanisms were first hypothesised by Hermia [23] and further developed for cross flow filtration by Field et al. [24] to account for solute removal from the membrane surface by introduction of a limiting flux term. Fitting of empirical flux data to the power-law equations in terms of powers of n gives a qualitative assessment to the mechanism of blocking occurring at a given time during flux decline, whether it be cake filtration ($n = 0$), standard blocking ($n = 1$), intermediate blocking ($n = 1.5$) or complete blocking ($n = 2$). A diagrammatic illustration of the pore-blocking mechanism can be seen in Fig. 2. The model is mathematically described by the following ODE (Eq. (1)).

$$-\frac{dJ}{dt}J^{n-2} = k_b(J - J^*) \tag{1}$$

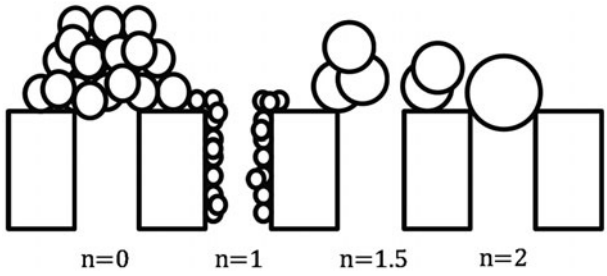

Fig. 2. Pore blocking mechanisms.

where J is the flux at a given time t, n is the mechanism specific power, and k and J^* are the mechanism specific flux decline constant and limiting flux, respectively. Whilst the outcome of such models can be somewhat speculative, they do present insightful understanding to the filtration problem and are of use in influencing latter decisions with regard to selection of operating conditions.

2. Experimental

2.1. Filtration apparatus

Experiments were carried out on a DSS LabUnit M-10 filtration system (DSS, Silkeborg, Denmark) equipped with an inline gear pump (ECO Gearchem, Pulsafeeder, NY, USA), shell and tube heat exchanger (Alfa Laval, Nakskov, Denmark) connected on the shell side to a water bath. System flow rate was monitored using a rotameter. Solutions were contained within a 10 L glass feed tank (Soham Scientific, Soham, UK). Permeate mass was measured gravimetrically. Pressure and line temperature was monitored using pressure transducers (Druck, Leicester, UK) and thermocouple positioned at the module inlet. All data was sent via a remote data acquisition module (ADAM-4012, Advantech, Milpitas, USA) to LabView software v.10.0 (National Instruments, Austin, USA) where mass/time and temperature were used to calculate permeate volumetric flux. The membrane module was a DSS LabStack M-10 module consisting of 4 polysulphone plates in a plate and frame arrangement, each plate housing a single membrane coupon of 8.4×10^{-3} m^2 area, giving a total effective filtration area 0.0336 m^2.

2.2. Membranes

Synthetic membranes supplied by Alfa Laval, Nakskov, Denmark were cut from a roll to the required size and mounted into the module. Prior to all filtrations, water was fluxed through at 60˚C for 90 min at 1.0 bar transmembrane pressure (TMP) and 1.5 ms^{-1} cross flow velocity (CFV) to remove a glycerol anti-humectant applied by the manufacturer. The membranes investigated were all of hydrophilic asymmetric type with polysulphone active layers and polypropylene support layers. Manufacturer (Alfa Laval, Nakskov, Denmark) product codes were: GRM RT5, PSU RT1 and PSU RT8, corresponding, respectively, to 0.5, 0.9 and 1.5 μm nominal pore size and are coded in this article as PS05, PS09 and PS15. Pure water flux (J_{PWF}) was taken at room temperature (RT) enabling calculation of membrane intrinsic resistance (R_m), calculated following temperature, that is viscosity (μ) correction using Eq. (2).

$$J_{PWF} = \frac{TMP}{\mu R_m} \quad (2)$$

2.3. Black tea powder

CWS spray-dried tea powder was from a Kenyan plantation and kindly supplied by *James Finlay Ltd*. Tea was reconstituted at RT using reverse osmosis (RO) water agitated by a stirrer at 500 rpm for 20 min. Tea was stored in separate 1.0 kg quantities; weighing and reconstitution proceeded as per requirement within an hour prior to filtration. A feed volume of 8 L was used for all experiments.

2.4. Filtration experiments

After initial PWF measurement, filtration of 10.0 wt.% tea was carried out at RT and a range of TMPs (1.0–4.0 bar) at 1.0 ms^{-1} CFV for 1 h with permeate being recycled back to the tank upon collection (excluding samples). After 1 h, the system was purged with RO water at the minimum allowable CFV and TMP. Following this, RT RO-water was fluxed through the membrane for 15 min at 1.5 ms^{-1} CFV and 1.0 bar TMP to rinse off loosely bound foulant material. Cleaning of membranes was carried out at 60˚C with 0.5 wt.% NaOH dissolved in RO water, using 1.5 ms^{-1} CFV and 1.0 bar for 10 min before a final system purge and measurement of the PWF at RT once again. New membranes were used for each set of experimental conditions so as to maintain consistent fouling conditions. Experiments with 1.0 and 5.0 wt.% feed concentration were carried out for PS09 and PS15 so as to ascertain fouling mechanisms during fouling and to give estimates of mass transfer coefficients (MTCs) as explained by Eq. (3). Further to this, the effect of CFV was assessed for PS09 and PS15 by carrying out 1.0 bar TMP filtration of 10.0 wt.% tea at 0.5, 0.8, 1.0 and 1.5 ms^{-1}.

2.5. Total solids

Sample concentration was calculated by dehydration at 70˚C. Ten-millilitre test tubes were weighed prior to the addition of ~8 mL of sample. After weighing again, samples were dried in an incubator at 70˚C for 5 d. Sample tubes were then re-weighed and returned to the incubator. After a subsequent day, samples were again re-weighed to check full dehydration and, upon confirmation, enabled total solids concentration of samples to be calculated. For all filtrations, samples were taken at 15, 30, 45 and 60 min and analysed in triplicate.

2.6. Total polyphenols

Polyphenols concentration was measured using a modified method as described by Singleton and Rossi for colourimetric determination of polyphenols [25]. The method was adapted for use in microtitre plates with the linear range confirmed by calibration against known concentrations of gallic acid (GA). GA (Sigma Aldrich, Poole, Dorset) stock solutions were made up from a 1.0 mg mL^{-1} stock in serial dilutions of concentration between 0 and 50 μg mL^{-1}. Tea samples were diluted by half and then mixed with acetonitrile (ACN) (Fisher Scientific, Loughborough, UK) in the ratio 1.8 mL/0.2 mL (sample/ACN). one part sample/ACN mixture was further diluted in nine parts water; then 50 μL of this dilution (and the same of GA serial dilutions) were added to microtiter wells containing 100 μL Folin and Ciocalteu reagent (Sigma Aldrich) with prior 10-fold dilution. After 2–8 min, 80 μL of 7.5 wt.% sodium carbonate was added to each well. Plates were incubated for 8 h at RT prior to absorbance measurement at 765 nm using a Synergy HT multi-mode microtiter plate reader (BioTek Instruments, Winooski, USA). Samples were taken from the same time points during filtration as for the total solids samples and analysed in quadruplet.

2.7. Rejection coefficient of solutes

Using feed/retentate and permeate stream concentration for total solids and polyphenols, rejection coefficients for the given solute category was calculated by Eq. (3).

$$R_{\text{app}} = 1 - \frac{c_{p,i}}{c_{r,i}} \tag{3}$$

where R_{app} is the apparent rejection coefficient of solute i. c_p and c_r are concentrations of permeate and feed/retentate streams, respectively.

2.8. Refractive index

Refractive index was quantified in terms of Brix using a digital handheld refractometer (r^2 Mini, Reichert, NY, USA). The measurements provided an online concentration measurement enabling suitable dilutions to be made so as to ensure consistent concentrations when making subsequent turbidity and colour measurements. Readings have not been produced in this article, given the more precise dry weight measurements available. They were purely an intermediary means of fast sample screening before dilution.

2.9. Tea dilution

Tea was diluted with water and citric acid to simulate "in-bottle" conditions and mimicking pH adjustment in an RTD tea beverage. Tea sample Brix measurements were used to dilute tea samples from their bulk feed/retentate and permeate concentrations. Ten millilitres of 3.0 wt.% citric acid was added with the necessary volume of tea to produce 100 mL of 0.3 wt.% tea when water was added. The protocol was developed through personal correspondence. The result of adding citric acid in such high concentrations induces significant haze formation in the diluted tea product allowing for a robust test of the membrane's de-hazing capability.

2.10. Turbidity

Haze of tea samples was quantified in terms of sample turbidity at RT. Tea samples were loaded into a glass cuvette and mounted in a turbidimeter (model HI 93703, Hanna Instruments, Woonsocket, USA). The instrument was 3-point calibrated using turbidity standards of 0, 10 and 100 nephelometric turbidity unit (NTU). For stability over time, samples were stored at 5˚C. Prior to measurement, sample were allowed to equilibrate to RT and gently agitated to allow suitable mixing of any settled aggregates. After measurements, remaining sample was returned to cold storage. The measured sample was discarded.

Fig. 3 shows the formation of haze over time. The target maximum turbidity for the filtered product is below 50 NTU as denoted by the dashed line.

2.11. Colour

CIELab tristimulus colour coordinate measurements were made by detection of transmitted light in the visible spectrum (from 380 to 770 nm was used here). The diluted samples were transferred into 10-mm path-length cuvettes (Fisher Scientific) and loaded into a Shimadzu UV-1601 spectrophotometer

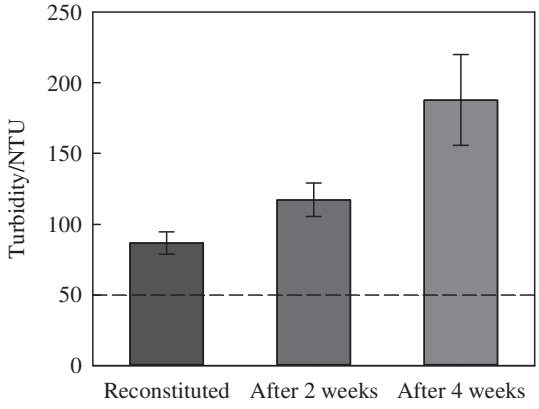

Fig. 3. Turbidity and haze formation for 0.3 wt.% unfiltered reconstitute in 0.3 wt.% citric acid at RT (stored at 5°C) (dashed line is target turbidity).

(Shimadzu Corporation, Kyoto, Japan). After transmittance measurement, UVPC Color Analysis software v.3.0 (also Shimadzu) converted the readings to L^*, a^* and b^* coordinates. Samples were measured in triplicate with mean and standard deviation providing the measure and error accordingly.

2.12. MTC calculation

With knowledge of R_{app} at various concentrations and the associated filtration fluxes, calculation of experimental MTCs was made using classical film theory by rearrangement of the CP model for solute back-diffusion away from the membrane surface and substitution of Eq. (3) to gain the expression:

$$\ln\frac{R_{app}}{1-R_{app}} = \ln\frac{R_{max}}{1-R_{max}} + \frac{J}{k} \tag{4}$$

where R_{max} is the actual rejection coefficient of solute at the membrane surface, given the increased concentration in this region as a result of CP. k is the MTC acting over the CP boundary layer; this relates the diffusion coefficient D to the boundary layer thickness δ through the following expression:

$$k = \frac{D}{\delta} \tag{5}$$

2.13. Resistance calculation

Membrane resistance during fouling and at the initial and final stages of rinsing allowed estimation of specific resistances arising as a result of CP effects (R_{CP}), reversible fouling (R_r) and irreversible fouling (R_i). By expansion of the resistance term in Eq. (2) to account for the effect of fouling and CP, the following equation is obtained:

$$J = \frac{\text{TMP}}{\mu(R_m + R_f + R_{CP})} \tag{6}$$

where R_f is the resistance to fouling ($R_f = R_i + R_r$). By subtraction of the resistance during filtration (total resistance, termed R_T) from the initial rinsing flux, an estimation for the resistance due to CP can be made ($R_{CP} = R_T - R_{rinse,initial}$). The reversible (or rinsable) fouling resistance (R_r) can then be estimated by subtraction of resistance due to CP and the resistance at the end of rinsing from the total resistance during filtration ($R_r = R_T - R_{rinse,final} - R_{CP}$). Fouling resistance is then calculated by subtraction of the intrinsic membrane and CP resistances from the total resistance ($R_f = R_T - R_m - R_{CP}$). Finally, irreversible fouling resistance (non-rinsable fouling) can be determined ($R_i = R_f - R_r$). All resistance terms are quantified in units of m^{-1}.

2.14. Determination of pore-blocking mechanism

Flux data were fitted to the four power-law mechanisms as described by Eq. (1) in terms of relative flux. The "fminunc" function in MATLAB R2012b was used and coupled with the inbuilt "ode45" differential equation solving routine to find solutions to Eq. (1). Curve fitting for each power n was carried out assessing both the determination coefficient (r^2) and sum of the square of the residuals as the criteria for assessment of the dominant pore-blocking mechanism.

3. Results and discussion

3.1. Membrane flux

Membranes process viability can be assessed in terms of flux although this is not the sole criteria as species selectivity/transmission is also of equal or greater importance. Quasi-steady-state fluxes were measured across a 1.0–4.0 bar TMP range after 60 min and are presented in Fig. 4. Limiting fluxes were approached for all membranes at 4.0 bar, the limiting values being approximately 10, 17 and 21 L m^{-2} h^{-1} for PS05, PS09 and PS15, respectively, as derived by fitting Eq. (6) to the data with prior knowledge of R_m.

Field et al. [24] and Howell [26] describe the situation in which the flux–pressure relationship is divided

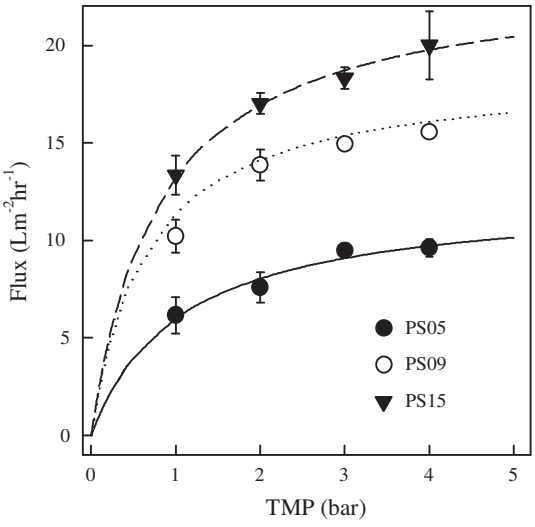

Fig. 4. Variation in flux with TMP.

into three regions, namely (i) sub-critical operation where flux increase is dependent upon the TMP and independent of membrane fouling, (ii) TMP is above a certain critical pressure and there is fouling-controlled flux which is thus a time-dependant flux and (iii) where TMP far exceeds the critical pressure and severe cake formation limits flux. With additional pressure, cake compression can lead to further declines in flux. Brans et al. [27] state that in region (ii), flux is independent of pore size, which is not the case here; however, the flux–pressure trend is not linear as would be the case in region (i). The results suggest that the working region is somewhere in the transition zone of region (i) and (ii).

Thus, there exists a region where both a flux–pressure dependency and the onset of fouling have occurred, with the formation of a dynamic cake limiting flux increase, which can be described by back-transport and gel filtration models [27]. The fluxes are still highly pore-size dependant implying cake filtration is not the sole or even dominating mechanism causing flux declines.

As already mentioned, data fits employ the resistance model, with the resistance causing flux decline expanded to account for back-diffusion (CP) and fouling layer build-up (both internally and as a cake) as shown in Eq. (6). The expression has been deemed suitable, given the laminar flow regime; these flow dynamics are unlikely to prolifically disturb the cake settling and resulting solute accumulation/deposition on the membrane surface. Also given, the high solids concentration indicates that back-diffusion from the cake/CP interface across the CP boundary layer and the associated resistance could be substantial.

By subtraction of R_m from the total resistance R_T, the sum of R_f and R_{CP} can be determined. The expanded resistance term is shown graphically in Fig. 5. The combined resistance shows a linear increase with TMP. The quantitative breakdown of this term is calculated and discussed later.

3.2. Solids transmission

Total solids transmission by dry weight measurement of feed and permeate samples was carried out after 1 h of filtration (at the same instant as quasi-steady-state flux assumptions). The trend observed is that of a negative linear correlation with TMP increase ranging from ~79% transmission at 1.0 bar to ~69% transmission at 4.0 bar for PS15 in the best case. In the worst case, transmission at 1.0 bar measured 61% and dropped to 42% over the same pressure range for the PS05 membrane as shown in Fig. 6.

The observation of increased rejection of solute with TMP has been noted by a number of authors. Visvanathan and Ben Aim [28] reported that a rejection increase both over processing time and with increased TMP was significant during MF of ~12 nm silica colloids. Blanpain et al. [29] also noted that when TMP was stepped from 10 to 100 kPa, increased rejection was recorded during MF of lager beer solutes, although for the filtration scheme in the given article (dead-end stirred), the effect of retentate concentration cannot be ruled out as effecting the rejection, despite the presence of an excess feed reservoir. These findings are indicative of this process, with both authors pointing towards the theoretical hypothesis

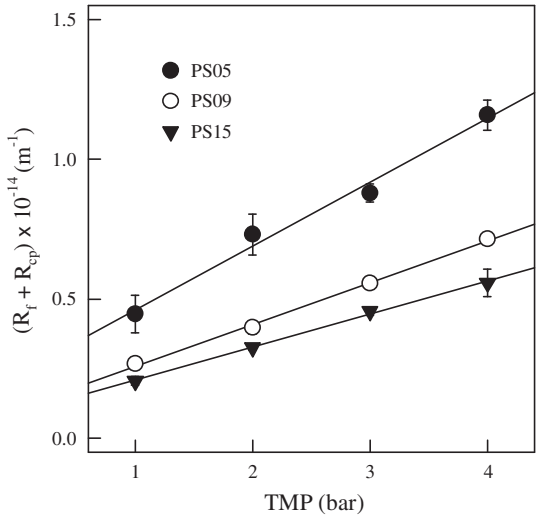

Fig. 5. Combined resistance caused by fouling and CP.

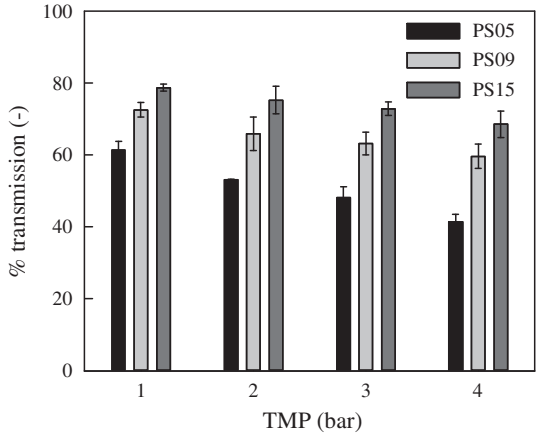

Fig. 6. Transmission of total solids.

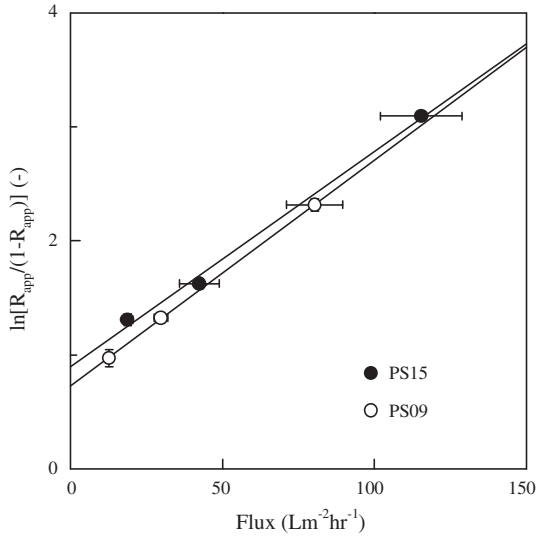

Fig. 7. Determination of maximum rejection coefficient and MTCs.

that in the early stages of filtration, pore constriction (through a standard blocking mechanism) acts to reduce the effective pore diameter (internal fouling), followed by the onset of a surface cake acting as a composite membrane (external fouling) due to protein–membrane interactions [29]. With higher pressures, cake layer compaction occurs and increased CP is in effect, resulting in a raised rejection of the composite membrane due to the now effective "tighter" pores.

3.3. Mass transfer

Concentration was varied in order to determine experimental MTCs for total solids with a view to aiding future process design. 1.0, 5.0 and 10.0 wt.% were filtered through PS09 and PS15 membranes with solids transmission being monitored at the quasi-steady-state point. PS05 was excluded from this experimentation due to the low (unacceptable) loss of solutes recorded during flux measurements with varied TMP.

By calculation of R_{app} and plotting against J (Fig. 7), the integrated form of the boundary layer model (Eq. (4)) was used to deduce the gradient of the line (and thus deduction of k) and the intercept, in order to estimate R_{max}, so as to allow calculation of the concentration at the membrane surface (c_m). Experimentally measured and derived values are displayed in Table 1. This method was the same as used by Evans and Bird when estimating the MTCs for black tea UF with feed concentrations of 0.5–1.5 wt.% [19].

The calculations in Table 1 show that there is marginally better mass transfer through the PS15 membrane as could be deduced from rejection coefficients. If Eq. (5) is considered, for constant back-diffusion and mass transfer, that is at steady state conditions, boundary layer thickness will be slightly greater for the PS09 than PS15 membrane, meaning the performance is hindered more due to CP for the smaller-pore-size membrane and a factor in the causation for the lower observed fluxes, even though the driving force (concentration gradient) in the back-diffusive boundary layer is greater for the PS15 membrane.

Overall, the findings provide evidence that a concentration gradient over a boundary layer plays an important role in limiting fluxes during tea filtration despite the presence of large and inconsistently sized particulates. For these reasons, it is advantageous to work at sub-critical fluxes (lower TMP) although in practice, working at TMPs which are low enough to be sub-critical leads to unacceptably low fluxes.

3.4. Resistance-in-series model

Resistance breakdowns were quantified as previously explained using Eq. (6). Calculations show that resistances during fouling were dominated by CP for all membranes as shown in Fig. 8. An increase in R_{CP} from $1.57 \times 1.0^{13} \pm 1.92 \times 1.0^{12}$ to $8.19 \times 1.0^{13} \pm 3.24 \times 1.0^{12}$ for the PS05 membrane between 1.0 and 4.0 bar represents over a fivefold increase, and this magnitude of increase being repeated for PS09 and PS15 also.

Another trend noticeable is that of the transition from rinsable fouling at lower TMP to irreversible fouling at higher TMP, shown clearly for PS05 membrane. This shows that as pressure is built up on the cake layer, the compaction forces material to foul

Table 1
Maximum rejection coefficients, membrane surface concentration and MTCs

Membrane	J (L m^{-2} h^{-1})	c_r (% wt./wt.)	c_p (% wt./wt.)	R_{app} (–)	R_{max} (–)	c_m (% wt./wt.)	$k \times 10^{-5}$ (ms^{-1})
PS09	80.3 ± 9.2	2.01	1.83	0.090	0.326	2.59	1.40
	29.7 ± 2.3	4.99	3.94	0.210		5.54	
	12.6 ± 0.5	9.54	6.92	0.275		9.74	
PS15	115.4 ± 13.3	1.95	1.86	0.043	0.289	2.62	1.47
	42.3 ± 6.5	5.12	4.28	0.165		6.02	
	18.7 ± 1.7	9.76	7.68	0.213		10.81	

more prominently on the membrane surface which then transitions to non-rinsable fouling (irreversible) when subjected to the same applied shear force during the rinse cycle and thus would require stronger chemical treatment for removal. The relative magnitude of irreversible fouling to total fouling resistance also increases noticeably for PS09 and PS15 membranes, although these are dominated by the size of resistances due to CP, especially at elevated pressures. This does not appear to be a substantially significant increase in the absolute sizes of rinsable fouling for the PS15 membrane and only a slight increase in irreversible fouling magnitude. It is R_{CP} in all cases which plays the dominant role in retarding flux suggesting that the linear trend observed in Fig. 5 is strongly dependant on this resistance, as is also apparent from the resistance breakdowns.

3.5. Effect of CFV

CFV was varied in the apparatus' workable range from 0.5–1.5 ms^{-1} at 1.0 bar TMP. Additional CFV was successful in changing steady state fluxes from 7.3 ± 1.1 to 12.2 ± 0.5 L m^{-2} h^{-1} for PS09 and 8.5 ± 0.9 to 16.4 ± 2.0 L m^{-2} h^{-1} for the PS15 as shown in Fig. 9(a). Increases in CFV are known to induce greater shear forces on the membrane or surface layer acting to mediate cake growth.

Also in effect are increased solids transmissions (Fig. 9(b)), and for PS09, it ranged from 58 ± 2 to 84 ± 6%, and for PS15, it measured from 70 ± 3 to 81 ± 1%. Head and Bird [30] reported the same effect when filtering high solids content milk protein isolate for the removal of spores noticing a solids transmission increase from 6.4 to 10.7% and also an increased protein transmission of 15 to 19% when filtering with a 1.4-μm ceramic membrane at CFV values of 0.7 and 1.4 ms^{-1}, respectively. Van der Berg et al. [31] stated that $k \propto CFV^{0.33}$ when operating in the laminar regime (as is the case here with Reynolds numbers between ~520 and ~1,560). The changes in flux monitored here suggest changing the CFV can affect performance significantly; however, apparatus modification would be required to gain CFVs whereby the flow regime is in the turbulent region, that is Re > 2,300, for more viscous feeds such as the concentrated tea.

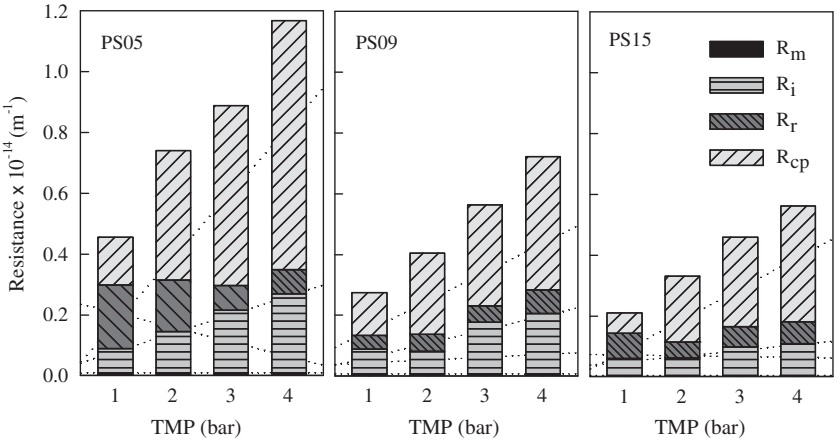

Fig. 8. Resistance break-downs for all membranes.

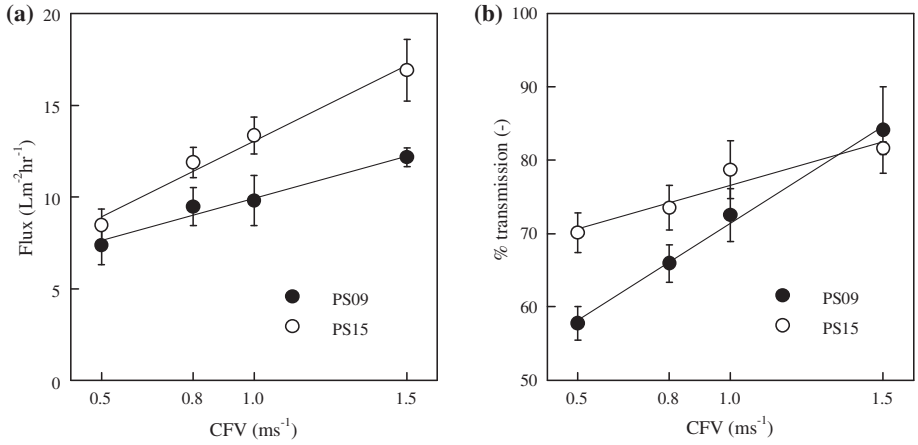

Fig. 9. Effect of CFV on (a) flux and (b) solids transmission at 1.0 bar TMP.

3.6. Pore-blocking mechanisms

Data fits of the classical pore-blocking laws were carried out for 1.0, 5.0 and 10.0 wt.% flux decline data as shown in Fig. 10 using a methodology in accordance with Giorno et al. [32] and De Barros et al. [33] whereby the limiting flux during fitting was taken as the quasi-steady-state filtration flux. The data (Fig. 10(e) and (f)) show that there is an almost instantaneous flux decline when using 10.0 wt.% tea which most closely fits the complete ($n = 2$) blocking law ($r^2 = 0.853$) for PS09 and cake filtration law ($n = 0$) for PS15 ($r^2 = 0.930$) over the filtration duration. Given such a high solids load in the bulk, and an even greater concentration at the membrane surface when CP is considered, it would be assumed that the sudden flux decline is likely due to an almost instant deposition of solids and corresponding cake build-up. Given also that tea cream and aggregation is adversely affected by high concentration, it could be assumed that the fouling build-up at the membrane surface would be in some way analogous to that of creaming of tea in bulk solution, although this time, deposition could be worsened by attachment (adsorptive fouling) of species to the membrane surface. Target species for this effect would be polyphenols given they are highly hydroxylated and partially soluble, with specific TFs shown to be predominant in tea fouling behaviour [22] or caffeine, again only partially soluble and exhibiting hydrophobicity resulting in apolar interactions in solution [34].

Considering 1.0 wt.% filtration for PS09, a clear transition from complete pore blocking in the early stages of filtration to cake filtration as the filtration progresses is shown in Fig. 10(a). This behaviour was also observed by De Barros et al. [33] when observing pineapple juice filtration using hollow fibre PS membranes. The effect occurs more rapidly when using 5.0 wt.% tea (Fig. 10(c)). It would be safe to assume that even though the cake filtration mechanism does not adequately describe the filtration scenario for 10.0 wt.% tea, instantaneous cake deposition for the high concentration is a near certainty, at least when compared to the other blocking mechanisms, even if a "sharp" flux decline regime is best described by complete pore blocking. There appears to be a lack of understanding of this phenomenon in the literature.

3.7. Haze removal

Following filtration and suitable dilution to 0.3 wt.% with 0.3 wt.% citric acid, tea turbidity was measured directly after filtration and then again after 2 and 4 weeks. The results shown in Fig. 11 indicate that for the PS05 membrane, haze removal is superior over PS09 and PS15. This would be expected given the smaller pore diameter and thus better efficiency in separating out haze aggregates. There was no significant change in the haze for all TMPs tested directly after filtration for PS05. Counter intuitively, operating at a lower TMP was found to reduce haze more efficiently than operating at higher TMP. This is the opposite of what was indicated by the solids transmission data. These findings suggest that haze-causing aggregates can transmit through the membrane (and cake layer) more readily than other solutes with these membrane pore sizes. Reasoning for this could be that aggregates would be transmitted to the membrane surface through convective flow as like any other solute. With the presence of the CP boundary layer, diffusion of these larger aggregates would be lower (due to their greater hydrodynamic radius) than smaller unassociated solutes, according to the Stokes–Einstein equation. This would result in an overall greater

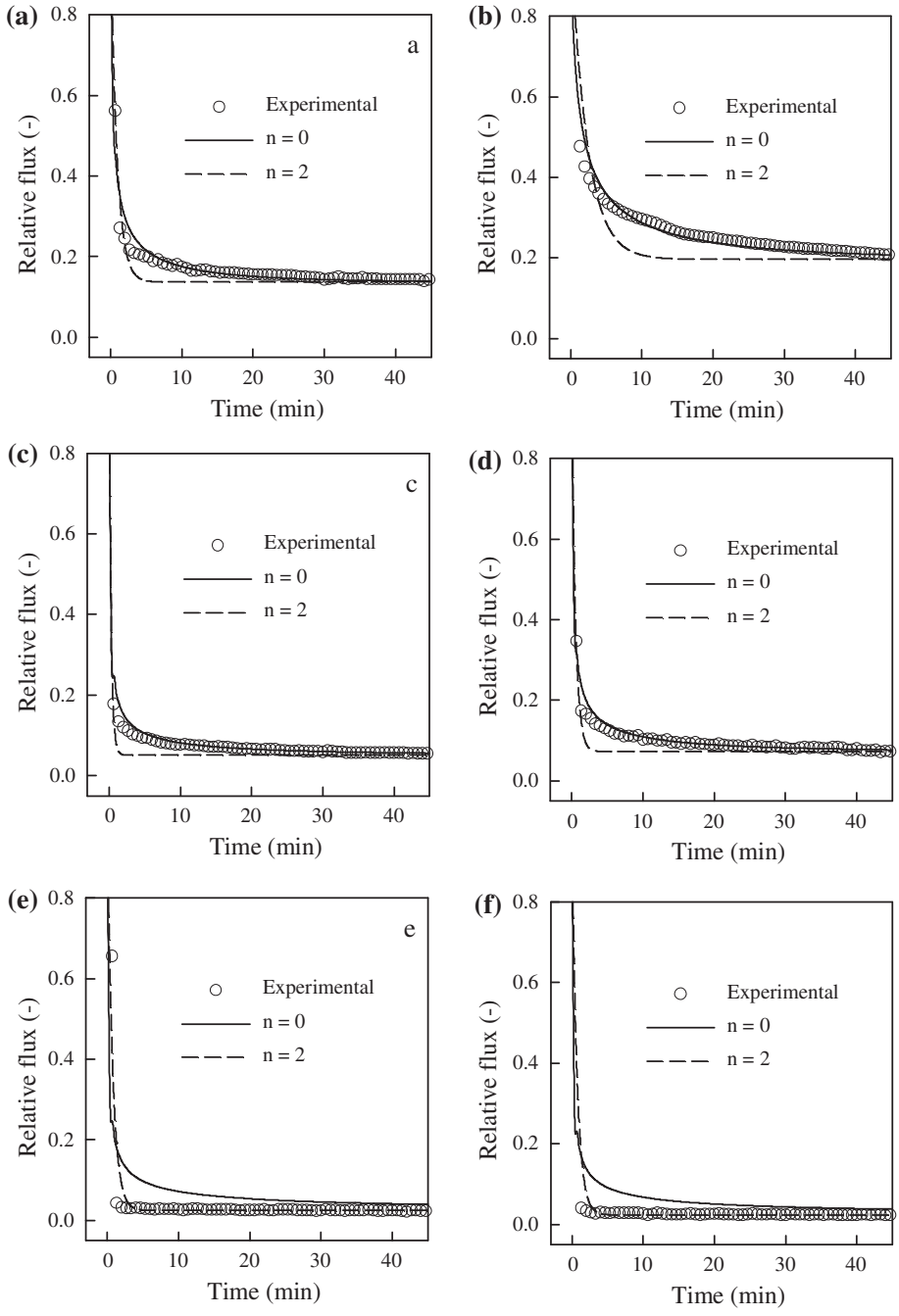

Fig. 10. Pore blocking mechanism fits for (a) PS09—1.0 wt.%, (b) PS15—1.0 wt.%, (c) PS09—5.0 wt.%, (d) PS15—5.0 wt.%, (e) PS09—10.0 wt.%, and (f) PS15—10.0 wt.%.

concentration at the membrane surface of aggregates to unbound solutes as smaller unassociated solutes would diffuse back into the bulk solution more readily, presenting a higher chance of transmission. At elevated TMP, this effect would be increased given the more pronounced effect of CP as shown by previous resistance breakdowns.

Given the relatively constant ageing turbidity over the TMP range for PS05, and the varying result for PS09 and PS15, the suggestion that the PS05 is creating a more robust barrier to haze aggregates (through size exclusion) is reaffirmed, whereas the counterpart membranes rely more on the composite "membrane" fouling layer (i.e. cake) to achieve separation. As

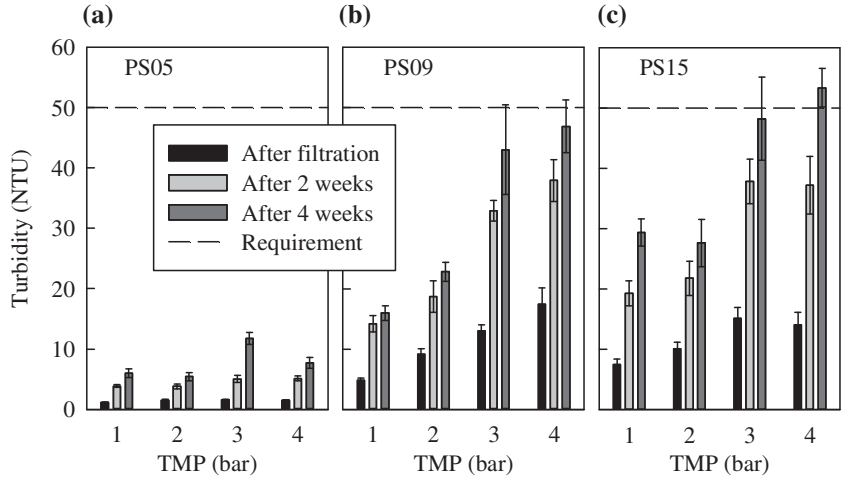

Fig. 11. Turbidity of permeates following membrane filtration.

stated previously, measurement from light scattering experiments indeed showed that tea cream aggregates were prolific around the 0.5-μm size range which further reaffirms this hypothesis [15].

Fig. 11 also shows the quantitative analysis of haze reformation over time at various TMPs. Haze reformation for PS05 membrane (Fig. 11(a)) remains low after 4 weeks in comparison with PS09 and PS15 (Fig. 11(b) and (c)). The sample with most clarity (1.0 bar TMP for PS05) rises from 1.1 ± 0.1 to 6.0 ± 0.7 NTU and the 4.0 bar (lowest initial clarity for PS05) rises from 1.5 ± 0.1 to 7.7 ± 0.9 NTU. Haze reformation is greatly increased as pore size increases. In the least effective instances (at 4.0 bar for PS09 and PS15), haze rises from 17.5 ± 2.7 and 14.1 ± 2.1 NTU to 46.9 ± 4.3 and 53.4 ± 3.0 NTU for the respective membranes. These haze reformation results would not entirely satisfy the producer's requirements. The PS09 and PS15 membranes do perform to an adequate standard at lower TMPs, where turbidity rises from 4.9 ± 0.3 to 16.0 ± 1.2 NTU (for PS09) and 7.5 ± 0.9 to 29.4 ± 2.2 NTU for PS15 (both changes being for 1.0 bar TMP).

The kinetics of haze formation has been shown by Siebert with results showing for grape juice, cranberry juice and apple juice a plateau phase over the initial time course (~20 d), and then, a sharp increase in turbidity [35]. McMurrough et al. show that with lager beer the plateau region is shorter and chill haze formation begins much earlier (within 2 d) [36].

The data collected suggest that there appears to be a critical maximum turbidity value at which haze reformation is substantially reduced—achievable with the PS05 membrane. This value occurs around 2–3 NTU for freshly filtered tea streams, and above this value, haze reformation occurs more prolifically over time. Determining this value would require more refinement by reducing the mesh size for the experimental procedure and likely requiring the introduction of more process variables, although this was not within the scope of this study. Understanding how this value can be related to the chemistry of the constituents would require a more rigorous understanding of the binding capabilities of the given components, aggregate growth kinetics and the resulting partitioning characteristics of the cream phase and soluble phase.

Penders et al. showed from their light scattering studies of tea creaming that hydrodynamic radius of particles increases over time implying small tea cream particles accumulate in size over time [37]. With this in mind, expulsion of already formed tea cream particulates from the permeate side of the membrane will not only reduce haze in the short-term, but retard the long-term formation. Results from this study (substantively for PS05) reinforce these findings.

3.8. Permeate lightness and colour

Tea colour and haze were measured by absorbance across the visible spectrum. Results show that after dilution of the tea, lightness was higher for permeate of the smaller-pore-size membranes (Fig. 12). Wu and Bird attributed a darker tea to a better quality product with more total TFs present [22]. The lightness data collected here show progressive lightening with increased TMP, indicating that tea filtered at higher pressure has a greater proportion of TFs removed. Also, noteworthy is the lightness increase over the duration of the filtrations. This indicates that as foulant built up on the surface of the membrane, lower transmission of TFs occurred.

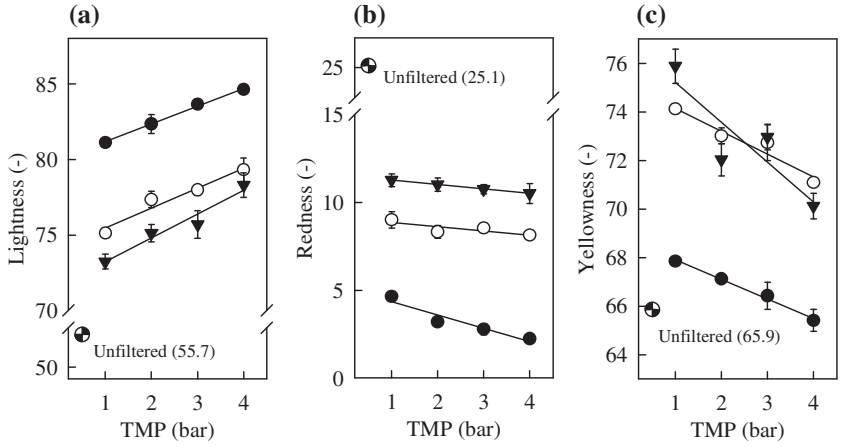

Fig. 12. (a) Lightness, (b) redness, and (c) yellowness of 0.3 wt.% tea permeate samples. ●—PS05, ○—PS09, ▼—PS15.

Liang and Xu assert that redness and yellowness [38] (or more generally orange colour [39]) are correlated to TF content. In a sensory evaluation performed by the aforementioned authors, positive correlations were drawn between appearance and quality (TFs content shown to be an indicator of this), as well as greater TFs concentration giving higher scores for aroma and taste perception. Fig. 12 also shows a^* and b^* colour coordinates measured for MF permeates. There is an overall loss in red (a^*) (Fig. 12(b)) and increase in yellow (b^*) (Fig. 12(c)) for all permeates compared with the unfiltered feed (a^* = 25.3, b^* = 65.9 for 0.3 wt.% tea reconstitute). The effect of an increase in TMP results in a lower red and yellow species transmission. At 4.0 bar filtration using the PS05 membrane, there is a slight loss in yellowness observed. Scharbert et al. also indicate that TRs produce the red-brown pigmentation in tea brews, which would contribute to a darkening of the tea brew [39]. Wu and Bird showed that when filtering tea component mixtures, TRs led to higher levels of fouling of UF membranes and greater levels of TFs rejection as a result [22]. This observation a posteriori would lead to a more yellow, less red and lighter tea due to selective transmission of species.

3.9. Total polyphenols

Total polyphenols content was measured as a complimentary technique to monitor tea quality in reinforcement to the colour losses found. The findings presented (Fig. 13) show that there are disproportionately less polyphenols transmitting through the membrane, especially at lower pore size, to the total solids transmission. In the worst case (PS05 at 4.0 bar), only 28.1 ± 1.3% are transmitted when compared to 42% of solids. For the PS09 and PS15 membranes tested at 1.0 bar, 61.9 ± 4.7% and 60.2 ± 4.6% of total polyphenols are transmitted respectively, in comparison with 73 and 79% of solids for the two membranes respectively, under the same conditions. The results demonstrate that there is a preference for non-polyphenolic species to transmit the membrane even when polyphenols have generally lower molecular weights (especially catechins and TFs) than other solutes present in black tea such as proteins, polysaccharides and cellulosic plant matter. It was postulated by Wu and Bird when conducting UF experiments with TF/tea protein mixtures that the aggregation of the proteins and polyphenols species dominated the charge at the membrane surface, and upon cake layer deposition, increased the negative charge of the system to one greater than a membrane fouled solely by tea protein alone and thus restricting further polyphenol and

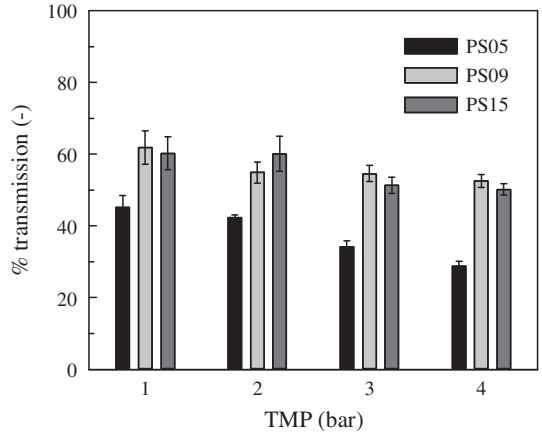

Fig. 13. Total polyphenols rejection for tea permeate samples.

protein transmission [22]. The authors also indicate that unbound TFs filtration fluxes displayed signs of high CP being in effect, another indicator for the preferential transmission of non-polyphenolic solutes.

Aside from the PS05 membrane, there was a marginal but insignificant increase in rejection between TMPs, suggesting that factors such as cake layer deposition, cake growth and CP may not be entirely responsible for the rejection of the majority of polyphenols and that interactions between the species and the membrane material itself are possibly the significant factors. These findings indicate that modification of membrane properties such as hydrophobicity and charge could help to reduce the shortfall in solute transmission.

4. Conclusions

MF has been shown to be effective in the haze removal and haze reformation of high solids content tea solutions. Filtrations showed variability in product quality, typically with a trade-off between acceptable solids transmission, haze reduction and flux. For all membranes examined, initially there was sufficient haze removal to satisfy the manufacturer's requirements, and the haze reoccurrence was significantly reduced, meaning there was successful enhancement of product quality as a result of the longer shelf life with respect to managing haze. The haze reformation of PS08 and PS15 membrane permeates did however rise to unacceptable levels after 4 weeks of cold storage. Further experiments are ongoing so as to ascertain whether storage temperature for membrane permeates is critical to haze reformation for the system studied here.

The high solids concentration of the feed resulted in both CP and cake filtration playing dominant roles in reducing flux. Nevertheless, fluxes at the lower end of what would be deemed industrially acceptable were gained, although efforts to maximise these fluxes by use of larger pore sizes resulted in lower haze removal, meaning the haze reduction efficiency decreased and rate of haze reoccurrence was increased. The PS05 membrane showed the greatest promise in terms of haze reduction although the high solids rejection meant that the total product loss was unacceptable.

Future work could examine regimes for the minimisation of product loss, such as constant and variable volume diafiltration. These would be promising candidates for this if the strict requirement for such a concentrated feed could be relaxed. Other aspects worth attention for batch processing operation are the application of tubular ceramic membranes operated at high CFV. These membranes are suitable for high solids load feeds as was demonstrated by Head and Bird for milk protein isolate in combination with backwashing [40]. CFV variation results for high solids load feeds also performed by Head and Bird [30] was shown to be a promising strategy in both maximising flux and minimising product loss. These strategies are likely to produce an improvement in the solids transmission values to those achieved in this study.

Acknowledgments

The authors thank the EPSRC for funding this research. We also thank Dr Frank Lipnizki (Alfa Laval, Nakskov, Denmark) for the donation of the membranes.

List of abbreviations

ACN	—	acetonitrile
CFV	—	cross flow velocity
CP	—	concentration polarisation
CTC	—	cut–tear–curl
CWS	—	cold-water-soluble
DSS	—	Danish separation systems
GA	—	gallic acid
MF	—	microfiltration
NTU	—	nephelometric turbidity units
PS	—	polysulphone
PWF	—	pure water flux
RO	—	reverse osmosis
RT	—	room temperature
RTD	—	ready-to-drink
TF	—	theaflavin
TMP	—	transmembrane pressure
TR	—	thearubigin
UF	—	ultrafiltration

List of nomenclature

a^*	—	redness parameter (CIELab colour space) (–)
b^*	—	yellowness parameter (CIELab colour space) (–)
c_p	—	permeate concentration (wt.%)
c_r	—	retentate concentration (wt.%)
c_m	—	membrane surface concentration (wt.%)
D	—	diffusion coefficient ($m^2\ s^{-1}$)
i	—	solute (–)
J	—	flux ($L\ m^{-2}\ h^{-1}$)
J^*	—	limiting flux ($L\ m^{-2}\ h^{-1}$)
k	—	mass transfer coefficient (ms^{-1})
k_b	—	blocking law constant (unit dependant on blocking mechanism)
L^*	—	lightness parameter (CIELab colour space) (–)
n	—	blocking mechanism index (unit dependant on blocking mechanism)
R_{app}	—	apparent rejection coefficient (–)
R_{max}	—	maximum rejection coefficient (–)

R_{CP} — resistance due to concentration polarisation (m^{-1})
R_f — resistance due to fouling (m^{-1})
R_i — resistance due to irreversible fouling (m^{-1})
R_m — intrinsic membrane hydraulic resistance (m^{-1})
R_r — resistance due to reversible (rinsable) fouling (m^{-1})
R_T — total resistance (m^{-1})
t — time
μ — dynamic viscosity (Pa s)
δ — thickness of concentration polarisation boundary layer (m)

References

[1] S. Li, C.-Y. Lo, M.-H. Pan, C.-S. Lai, C.-T. Ho, Black tea: Chemical analysis and stability, Food Funct. 4(1) (2013) 10–18.
[2] J.K. Tanui, W. Fang, W. Feng, P. Zhuang, X. Li, World black tea markets: Relationships and implications for the global tea industry, J. Int. Food Agribus. Market. 24(2) (2012) 148–168.
[3] D. Del Rio, L. Calani, F. Scazzina, L. Jechiu, C. Cordero, F. Brighenti, Bioavailability of catechins from ready-to-drink tea, Nutrition 26(5) (2010) 528–533.
[4] E. Jöbstl, J. O'Connell, J. Fairclough, M. Williamson, Molecular model for astringency produced by polyphenol/protein interactions, Biomacromolecules 5(3) (2004) 942–949.
[5] A. Noble, Astringency and Bitterness of Flavonoid Phenols, ACS Publications, Washington, DC, 2002, pp. 192–201.
[6] V. Sharma, L. Rao, A thought on the biological activities of black tea, Crit. Rev. Food Sci. Nutr. 49(5) (2009) 379–404.
[7] N. Khan, H. Mukhtar, Tea polyphenols for health promotion, Life Sci. 81(7) (2007) 519–533.
[8] L. Leung, Y. Su, R. Chen, Z. Zhang, Y. Huang, Z. Chen, Theaflavins in black tea and catechins in green tea are equally effective antioxidants, J. Nutr. 131(9) (2001) 2248.
[9] N. Kuhnert, J.W. Drynan, J. Obuchowicz, M.N. Clifford, M. Witt, Mass spectrometric characterization of black tea thearubigins leading to an oxidative cascade hypothesis for thearubigin formation, Rapid Commun. Mass Spectrom. 24(23) (2010) 3387–3404.
[10] C.S. Kumar, R. Subramanian, L.J. Rao, Application of enzymes in the production of RTD black tea beverages: A review, Crit. Rev. Food Sci. Nutr. 53(2) (2013) 180–197.
[11] N. Bhattacharyya, S. Seth, B. Tudu, P. Tamuly, A. Jana, D. Ghosh, R. Bandyopadhyay, M. Bhuyan, Monitoring of black tea fermentation process using electronic nose, J. Food Eng. 80(4) (2007) 1146–1156.
[12] V. Tolstoguzov, Thermodynamic aspects of biopolymer functionality in biological systems, foods, and beverages, Crit. Rev. Biotechnol. 22(2) (2002) 89–174.
[13] E. Jöbstl, J. Fairclough, A. Davies, M. Williamson, Creaming in black tea, J. Agric. Food Chem. 53(20) (2005) 7997–8002.
[14] Y. Liang, J. Lu, L. Zhang, Comparative study of cream in infusions of black tea and green tea, Int. J. Food Sci. Technol. 37(6) (2002) 627–634.
[15] Y. Liang, Y. Xu, Effect of pH on cream particle formation and solids extraction yield of black tea, Food Chem. 74(2) (2001) 155–160.
[16] D. Boadi, R. Neufeld, Encapsulation of tannase for the hydrolysis of tea tannins, Enzyme Microb. Technol. 28 (7–8) (2001) 590–595.
[17] S. Todisco, P. Tallarico, B. Gupta, Mass transfer and polyphenols retention in the clarification of black tea with ceramic membranes, Innovative Food Sci. Emerg. Technol. 3(3) (2002) 255–262.
[18] P.J. Evans, M.R. Bird, Solute-membrane fouling interactions during the ultrafiltration of black tea liquor, Food Bioprod. Process. 84(4) (2006) 292–301.
[19] P.J. Evans, M.R. Bird, The role of black tea feed conditions upon the ultrafiltration performance during membrane fouling and cleaning, J. Food Process Eng. 33(2) (2010) 309–332.
[20] P.J. Evans, M.R. Bird, A. Pihlajamäki, M. Nyström, The influence of hydrophobicity, roughness and charge upon ultrafiltration membranes for black tea liquor clarification, J. Membr. Sci. 313(1–2) (2008) 250–262.
[21] P.J. Evans, M.R. Bird, D. Rogers, C.J. Wright, Measurement of polyphenol-membrane interaction forces during the ultrafiltration of black tea liquor, Colloids Surf. A 335(1–3) (2009) 148–153.
[22] D. Wu, M. Bird, The fouling and cleaning of ultrafiltration membranes during the filtration of model tea component solutions, J. Food Process Eng. 30(3) (2007) 293–323.
[23] J. Hermia, Constant pressure blocking filtration laws-application to power-law non-Newtonian fluids, Chem. Eng. Res. Des. 60 (1982) 183–187.
[24] R. Field, D. Wu, J. Howell, B. Gupta, Critical flux concept for microfiltration fouling, J. Membr. Sci. 100(3) (1995) 259–272.
[25] V. Singleton, J.A. Rossi, Colorimetry of total phenolics with phosphomolybdic-phosphotungstic acid reagents, Am. J. Enol. Viticult. 16(3) (1965) 144–158.
[26] J.A. Howell, Sub-critical flux operation of microfiltration, J. Membr. Sci. 107(1–2) (1995) 165–171.
[27] G. Brans, C. Schroën, R. Van der Sman, R. Boom, Membrane fractionation of milk: State of the art and challenges, J. Membr. Sci. 243(1–2) (2004) 263–272.
[28] C. Visvanathan, R. Aim, Application of an electric field for the reduction of particle and colloidal membrane fouling in crossflow microfiltration, Sep. Sci. Technol. 24(5–6) (1989) 383–398.
[29] P. Blanpain, J. Hermia, M. Lenoël, Mechanisms governing permeate flux and protein rejection in the microfiltration of beer with a cyclopore membrane, J. Membr. Sci. 84(1–2) (1993) 37–51.
[30] L.E. Head, M.R. Bird, The removal of psychrotropic spores from Milk Protein Isolate feeds using tubular ceramic microfilters, J. Food Process Eng. 36(1) (2013) 113–124.
[31] G. Van den Berg, I. Rácz, C. Smolders, Mass transfer coefficients in cross-flow ultrafiltration, Journal of Membrane Science 47(1–2) (1989) 25–51.
[32] L. Giorno, L. Donato, S. Todisco, E. Drioli, Study of fouling phenomena in apple juice clarification by

enzyme membrane reactor, Sep. Sci. Technol. 33(5) (1998) 739–756.
[33] S. De Barros, C. Andrade, E. Mendes, L. Peres, Study of fouling mechanism in pineapple juice clarification by ultrafiltration, J. Membr. Sci. 215(1–2) (2003) 213–224.
[34] R. Martin, T.H. Lilley, N.A. Bailey, C.P. Falshaw, E. Haslam, D. Magnolato, M.J. Begley, Polyphenol–caffeine complexation, J. Chem. Soc., Chem. Commun. 2 (1986) 105–106.
[35] K.J. Siebert, Effects of protein-polyphenol interactions on beverage haze, stabilization, and analysis. J. Agric. Food Chem. 47(2) (1999) 353–362.
[36] I. McMurrough, R. Kelly, J. Byrne, M. O'Brien, Effect of the removal of sensitive proteins and proanthocyanidins on the colloidal stability of lager beer, J. Am. Soc. Brew. Chem. 50(2) (1992) 67–76.
[37] M.H. Penders, D.P. Jones, D. Needham, E.G. Pelan, Mechanistic study of equilibrium and kinetic behaviour of tea cream formation, Food Hydrocolloids 12(1) (1998) 9–15.
[38] Y. Liang, Y. Xu, Effect of extraction temperature on cream and extractability of black tea [Camellia sinensis (L.) O. Kuntze], Int. J. Food Sci. Technol. 38(1) (2003) 37–45.
[39] S. Scharbert, N. Holzmann, T. Hofmann, Identification of the astringent taste compounds in black tea infusions by combining instrumental analysis and human bioresponse, J. Agric. Food Chem. 52(11) (2004) 3498–3508.
[40] L.E. Head, M.R. Bird, Backwashing of tubular ceramic microfilters fouled with milk protein isolate feeds, J. Food Process Eng. 36(2) (2013) 228–240.